Scientific Research Report

Effect of Implant Angulation on Digital Impression Accuracy of Three-Unit Implant-Supported Restorations

Narges Ameri [a], *Mahnaz Arshad* [a,b], *Melika Ghaffari* [c], *Sareh Habibzadeh* [a,b*], *Seyed Ali Mosaddad* [d,e,f*]

[a] *Department of Prosthodontics, School of Dentistry, Tehran University of Medical Sciences, Tehran, Iran*
[b] *Dental Research Center, Dentistry Research Institute, Tehran University of Medical Sciences, Tehran, Iran*
[c] *School of Dentistry, Tehran University of Medical Sciences, Tehran, Iran*
[d] *Department of Research Analytics, Saveetha Dental College and Hospitals, Saveetha Institute of Medical and Technical Sciences, Saveetha University, Chennai, India*
[e] *Department of Conservative Dentistry and Bucofacial Prosthesis, Faculty of Odontology, Complutense University of Madrid, Madrid, Spain*
[f] *Department of Prosthodontics, School of Dentistry, Shiraz University of Medical Sciences, Shiraz, Iran*

ARTICLE INFO

Article history:
Received 7 January 2026
Received in revised form
14 March 2026
Accepted 17 March 2026
Available online 18 April 2026

Key words:
Dental implants
Dental impression technique
Computer-aided design
Computer-aided manufacturing
Prosthesis design
Dimensional measurement accuracy
Imaging
3-dimensional

ABSTRACT

Introduction and Aims: This study evaluated the effect of implant angulation on the accuracy of digital impressions for 3-unit implant-supported fixed partial dentures obtained with 2 intraoral scanners.

Methods: Three partially edentulous maxillary resin casts with 4 implants placed bilaterally at the first premolar and first molar sites were prepared with inter-implant angulations of 0° (parallel), 15°, and 30°. Scan bodies were attached and reference scans were obtained using an optical coordinate-measuring system. Each cast was scanned 12 times with 3Shape TRIOS 3 and CEREC Omnicam AC scanners. The datasets were superimposed onto the reference models, and linear and angular deviations were calculated. Data were analysed using generalized estimating equations (GEE) to evaluate the effects of implant angulation, scanner type, and implant pair.

Results: Implant angulation significantly affected digital impression accuracy. For linear deviation, the GEE model showed a significant cast × scanner interaction (β = 0.028; 95% CI, 0.017–0.039; $p < .001$). TRIOS 3 produced greater deviations than Omnicam at 0° and 15° (mean differences 0.029 mm and 0.018 mm), whereas it showed lower deviation at 30° (−0.027 mm). Linear deviations ranged from 0.50 to 0.68 mm. For angular deviation, no cast × scanner interaction was found (β = 0.017; 95% CI, −0.008-0.043; P = .078), but implant angulation had a significant effect (β = −0.628; 95% CI, −0.917 to −0.338; P = .001), with lower deviations at higher angulations (0.05°–0.06°). Scanner type and implant pair did not significantly affect angular accuracy.

Conclusions: Implant angulation influences the linear and angular accuracy of digital impressions for short-span implant-supported restorations. Within the limitations of this in vitro study, moderate implant angulations (15°-30°) did not adversely affect angular accuracy or compromise digital impressions of short-span implant configurations.

Clinical Relevance: Moderate implant angulation does not appear to compromise the accuracy of digital impressions of short-span implant-supported restorations, supporting the

* Corresponding author. Department of Prosthodontics, Tehran University of Medical Sciences. No.14, Heravi Sq., Zabeti St. Pasdaran Ave. Tehran, Iran; Department of Prosthodontics, School of Dentistry, Shiraz University of Medical Sciences, Shiraz, Iran.
E-mail addresses: sareh.habibzadeh@gmail.com (S. Habibzadeh), mosaddad.sa@gmail.com (S.A. Mosaddad).
Seyed Ali Mosaddad: http://orcid.org/0000-0001-6963-8289
https://doi.org/10.1016/j.identj.2026.109553
0020-6539/© 2026 The Authors. Published by Elsevier Inc. on behalf of FDI World Dental Federation. This is an open access article under the CC BY-NC-ND license (http://creativecommons.org/licenses/by-nc-nd/4.0/)

clinical use of intraoral scanners in situations where implant angulation is dictated by anatomical or surgical constraints.

© 2026 The Authors. Published by Elsevier Inc. on behalf of FDI World Dental Federation.
This is an open access article under the CC BY-NC-ND license
(http://creativecommons.org/licenses/by-nc-nd/4.0/)

Introduction

Dental implants are widely used for the replacement of missing teeth and have demonstrated predictable clinical performance in terms of function and prosthetic rehabilitation outcomes.[1,2] Achieving a passive fit between the prosthesis and the supporting implants is a fundamental requirement for the long-term success of implant-supported restorations.[3] Because dental implants lack a periodontal ligament, they cannot compensate for inaccuracies in prosthetic fit, and any misfit may increase stress on the implant–bone interface or prosthetic components.[4] Any misfit between the restoration and the implants may transfer excessive stress directly to the implant–bone interface or the prosthetic components, leading to biological or mechanical complications such as screw loosening, prosthetic fractures, or marginal bone loss.[5,6] Thus, obtaining an accurate impression is the first and most critical step toward fabricating a well-fitting restoration.[7] Various impression techniques have been developed to achieve an accurate master cast that ensures passive adaptation of the final prosthesis.[8]

However, in clinical practice, implant placement is often influenced by anatomical limitations or surgical constraints, leading to non-parallel or angulated implant positions.[9-11] Such angulations can complicate the prosthetic phase and compromise the impression's accuracy. Consequently, evaluating the accuracy of different impression techniques for both parallel and angulated implants is clinically relevant and necessary to ensure prosthesis longevity.

Despite improvements in materials and techniques, conventional impression methods still have disadvantages, such as patient discomfort, long working time, potential dimensional changes in impression materials, and human error during impression making or stone pouring.[12] To overcome these limitations, digital intraoral scanners (IOSs) were introduced to capture 3-dimensional virtual models of the oral cavity directly.[13] These systems eliminate the need for trays and impression materials, reduce the number of clinical and laboratory steps, and enhance patient comfort while maintaining high accuracy.[14] Digital impressions are also easily stored and transferred electronically to dental laboratories, promoting efficiency in the clinical workflow. However, the technology requires costly equipment and operator training, and its performance can vary depending on scanning principles and software algorithms.[15]

Over the past 2 decades, intraoral scanning technology has advanced significantly, enabling clinicians to obtain detailed, reproducible virtual models suitable for prosthetic design and CAD/CAM fabrication.[16,17] Nevertheless, the influence of implant angulation on the accuracy of digital impressions remains unclear. While several studies have shown that implant angulation of less than 15° does not significantly affect the accuracy of conventional impressions,[18-20] data regarding digital impressions remains limited. Furthermore, the impact of scanner technology on the capture of angulated implants has not been fully elucidated.

Among intraoral scanning systems, the CEREC Omnicam AC and 3Shape TRIOS 3 represent 2 well-established technologies based on different acquisition principles and have been extensively used in implant digital impression research. The CEREC system uses triangulation technology with continuous imaging and white LED light, while the TRIOS 3 system operates using confocal microscopy with ULTRAfast Optical Sectioning and confocal laser-scanning principles.[21-23] Although these systems are not the newest commercially available scanners, they remain relevant as representative platforms for evaluating the influence of scanner technology on impression accuracy. In addition, previous studies have reported inconsistent results regarding the effect of implant angulation on digital impression accuracy, and evidence remains limited for short-span 3-unit implant-supported restorations in which both linear and angular deviations are assessed under standardized experimental conditions.[24] Therefore, evaluating the behavior of these 2 established systems in a controlled short-span model may provide useful insight into the effect of implant angulation beyond a purely device-specific comparison.

This study aimed to evaluate the effect of implant angulation on the accuracy of digital impressions of implant-supported 3-unit fixed partial dentures obtained using CEREC and 3Shape TRIOS 3 scanners. The null hypothesis was that implant angulation and scanner type would not significantly influence the accuracy of digital impressions.

Materials and methods

This in vitro experimental study was approved by the Ethical Committee of the Tehran University of Medical Sciences (approval number: IR.TUMS.DENTISTRY.REC.1397.4922). Three pre-fabricated partially edentulous maxillary resin master casts were used in this study. Each maxilla was bilaterally edentulous at the first premolar and first molar sites. Dental implant fixtures (Bone Level Tapered; Ø 4.1 mm RC, 10 mm length; SLA® surface; Roxolid alloy; Loxim; Straumann Holding AG, Basel, Switzerland; REF No. 021.5510) were placed bilaterally at the first premolar and first molar sites with inter-implant angulations of 0°, 15°, and 30° in the first, second, and third casts, respectively. Divergent placement was used for the angulated implants. The implant angulations of 0°, 15°, and 30° were selected to represent clinically relevant implant positioning scenarios. A 0° configuration represents the ideal condition for parallel implant placement and is commonly used as a reference in implant accuracy studies. An angulation of approximately 15° reflects moderate implant divergence frequently encountered in clinical

practice due to anatomical constraints or prosthetic planning considerations. The 30° configuration was selected to represent a more pronounced yet clinically relevant divergence, similar to the angulations reported in tilted implant concepts such as the All-on-4 treatment protocol.[25] These angulation levels are also consistent with those used in previous studies evaluating the influence of implant angulation on impression accuracy.[9,26-30]

Sample size calculation

The required sample size was estimated using PASS 11 software (NCSS) for 2-sided pairwise comparisons with $\alpha = 0.05$, power = 0.80, and a standardized effect size (Cohen's d = 0.80), based on variability estimates reported by Giménez et al.[31] The analysis indicated a minimum of 12 scans per condition, which was adopted in this study.

Implant configuration

Implant osteotomies were prepared manually using a precision surveying device to achieve predetermined angulations relative to the implants' long axes. All angulations were defined with respect to the coronal portion of the implant using standardized anatomical directions. In Cast 1 (0°), all implants were placed parallel to the vertical axis. In Cast 2 (15°), implants B and C were each tilted 15° relative to the vertical axis in opposite anteroposterior directions, while implants A and D remained vertically oriented. In Cast 3 (30°), all implants were tilted 15° relative to the vertical axis, with implants A and B oriented in opposite anteroposterior directions and implants C and D oriented in opposite buccolingual directions, resulting in a total inter-implant divergence of 30° (Figure 1).

After preparation of the osteotomies, the dental implants were rigidly fixed in the resin casts using a high-strength autopolymerizing acrylic resin to prevent any positional movement. Implants were inserted under controlled conditions using the surveying device to maintain the predetermined angulations until complete polymerization of the resin. Implant stability was verified visually and manually after fixation. During data collection, implant positions were periodically rechecked, and no loosening or displacement of the implants was observed.

Digital impression procedure

Scan bodies (x, Ø 4.1 mm, H 10 mm, PEEK; Straumann Holding AG, Basel, Switzerland; REF No. 025.4915) were securely attached to the implants for each scan. After attachment of the scan bodies to the implants, the master casts were digitized using an optical coordinate measuring system (CMM; ATOS Compact Scan 5M, GOM GmbH) to obtain the reference dataset used for subsequent superimposition and deviation analysis. According to technical specifications for this system, the achievable point spacing ranges from approximately 0.02 to 0.3 mm, depending on the selected measuring volume and setup. Prior to scanning, the system was calibrated following the manufacturer's recommended procedure. The resulting dataset was imported into GOM Inspect (GOM GmbH) to obtain the reference spatial coordinates and inter-implant distances.

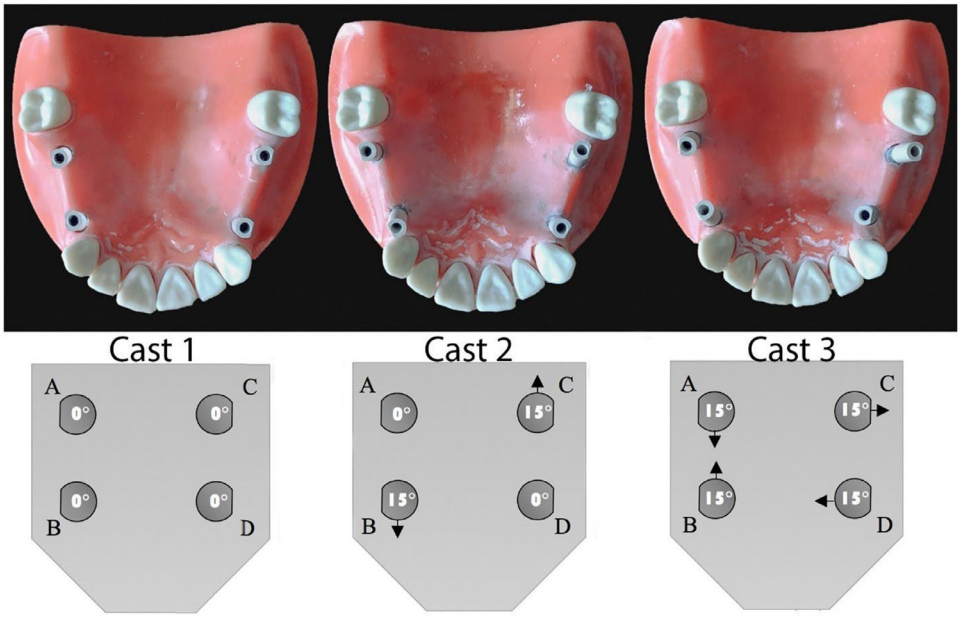


Fig. 1 – Implant angulation configurations of the experimental casts. Three experimental maxillary casts were prepared with inter-implant angulations of 0°, 15°, and 30°. In Cast 1 (0°), all implants were placed parallel to the vertical axis. In Cast 2 (15°), two implants were tilted 15° relative to the vertical axis in opposite mesiodistal directions, while the remaining implants were placed vertically. In Cast 3 (30°), all implants were tilted 15° relative to the vertical axis in opposing anteroposterior and buccolingual directions, resulting in a total inter-implant divergence of 30°.

For digital impressions, 2 intraoral scanners were used: 3Shape TRIOS 3 (3Shape, Copenhagen, Denmark) and CEREC Omnicam AC (Sirona Dental Systems GmbH). No surface powder was required, as the resin casts were fabricated with a matte surface that minimized reflection and enhanced optical capture.

Each scanner was calibrated before use according to the manufacturer's recommendations. Scanning was conducted under standardized ambient lighting by a single trained operator experienced with both devices. To capture the soft-tissue contours and running room around the implant sites, each cast was first scanned without the scan bodies. This initial scan ensured complete registration of the edentulous ridge and adjacent anatomical structures. After completion, the entire scanned surface was digitally locked in the scanner software to prevent the introduction of new data during subsequent scans. The scan bodies were then attached to the implants with their beveled surfaces oriented buccally to standardize their position across all scans. A second scan was performed, capturing only the scan bodies and their connection interfaces. This 2-step procedure ensured precise integration of the scan body geometry with the pre-existing cast surface without distortion or overlap.[29]

For both scanners, the scanning motion followed a standardized zigzag scanning path covering the entire cast arch.[32] Scanning began from the occlusal surfaces of the right posterior teeth, continued occlusally across the arch to the left side, and then proceeded along the buccal and palatal surfaces in a reverse direction to complete the arch. The scan bodies were finally rescanned from multiple angles to ensure complete capture of their geometry and accurate 3-dimensional registration.

To standardize scan body tightening across repeated disconnection and reconnection procedures, manual tightening was calibrated prior to data collection using a mechanical dynamometer. The manual tightening force applied by the operator was adjusted to correspond to a torque value of approximately 15 N·cm, and the same manual torquing protocol was consistently applied for all scans to ensure uniform seating of the scan bodies and minimize variability related to tightening force.

Each cast was scanned 12 times per scanner, resulting in 36 STL datasets per scanner across the 3 angulation configurations. To minimize potential order effects, the test scan sequence was randomized. The order of scanning the casts and the use of the scanner were randomized using a computer-generated random sequence (Microsoft Excel, Microsoft Corp.). This approach was applied consistently across all scanning sessions. The resulting Standard Tessellation Language (STL) files were exported for subsequent superimposition and deviation analysis in GOM Inspect software (GOM GmbH). To enhance methodological transparency and reproducibility, the key experimental parameters, scanning conditions, and calibration procedures used in this study are summarized in Table 1.

Superimposition and measurement

All STL files obtained from the intraoral scanners were imported into GOM Inspect software and superimposed onto the corresponding CMM reference models using the best-fit alignment algorithm. Alignment was performed using a best-fit algorithm applied to the entire surface geometry of the scan bodies. This approach was selected to maximize geometric constraint during superimposition and to reduce sensitivity to localized surface irregularities. Because the same scan body design, orientation (bevel facing buccally), and alignment protocol were applied consistently across all scans and for both intraoral scanners, any effects related to scanner resolution or surface sampling density were systematic and therefore unlikely to differentially influence inter-scanner or inter-angulation comparisons.

Each cast contained 4 implants (A–D) arranged from left to right across the maxillary arch, with implants A and B located at the left first premolar and first molar sites and implants C and D at the corresponding right-side sites. Two inter-implant pairs (A–B and C–D) were analysed within each cast. These pairs were evaluated separately to characterize pair-specific linear and angular deviations associated with their defined implant positioning and angulation configuration within the same experimental cast.

Within GOM Inspect, geometric features were constructed using controlled fitting procedures to limit the influence of surface noise and scanner-dependent resolution differences. Reference planes were generated by fitting a plane to a selected subset of the superior flat surface of each scan body, excluding edge regions and beveled transitions. The fitting regions were selected by the operator, whereas the reference planes were automatically calculated by the software using a least-squares algorithm. Plane fitting was performed using a least-squares approach with inspection of residuals to ensure acceptable fitting tolerance. The central longitudinal axis of each scan body was then derived by fitting a best-fit cylinder to the cylindrical portion of the scan body below the bevel region, rather than using the entire scanned surface. Similarly, although the cylindrical surface region was operator-defined, the best-fit cylinder and corresponding axis were computed automatically by the software using least-squares optimization. This approach minimized the influence of local surface irregularities and reduced geometric tolerance amplification associated with lower surface sampling density in intraoral scanner datasets. The intersection point between this axis and the reference plane was defined as the geometric center of the scan body and served as the reference point representing the implant position in the digital model (Figure 2). These reference centers were used to determine linear deviations, whereas angular deviations were derived from the orientation of the corresponding central longitudinal axes of the scan bodies representing each implant. The inter-implant distance was defined as the 3-dimensional Euclidean distance between the geometric centers of the scan bodies for each implant pair (A–B and C–D). Linear deviation was calculated as the absolute difference between the inter-implant distances measured in each intraoral scanner dataset and the corresponding distances obtained from the CMM reference model. Angular deviation was calculated by determining the difference in orientation between the central longitudinal axes of the scan bodies representing each implant pair in the test and reference datasets. Specifically, the angle formed between the axes of each implant pair was

Table 1 – Experimental parameters, scanning conditions, and calibration procedures

Category	Parameter	Description
Implant system	Implant system	Bone Level Tapered implants (Straumann Holding AG, Basel, Switzerland)
	Implant platform diameter	Ø 4.1 mm (Regular CrossFit platform)
	Implant length	10 mm
	Implant material	Roxolid® alloy
	Implant surface	SLA® surface
	Implant connection	Internal conical connection with CrossFit interface
	Implant placement sites	Bilateral first premolar and first molar positions
	Inter-implant angulation configurations	0°, 15°, and 30°
Scan body system	Scan body model	CARES® RC Mono Scanbody
	Manufacturer	Straumann Holding AG, Basel, Switzerland
	Scan body material	PEEK (polyetheretherketone)
	Scan body height	10 mm
	Platform compatibility	RC platform (Ø 4.1 mm)
	Scan body geometry	Cylindrical body with beveled orientation marker
	Orientation standardization	Beveled surface oriented buccally
	Tightening protocol	Manual tightening standardized to ∼15 N·cm
Reference digitization	Reference scanner	ATOS Compact Scan 5M optical coordinate measuring system (GOM GmbH, Braunschweig, Germany)
	Measurement principle	Structured blue-light optical scanning
	Point spacing	Approximately 0.02–0.3 mm depending on measuring volume
	Calibration	System calibrated according to manufacturer instructions before reference scanning
Intraoral scanners evaluated	Scanner systems	3Shape TRIOS 3 (3Shape, Copenhagen, Denmark) and CEREC Omnicam AC (Sirona Dental Systems GmbH, Bensheim, Germany)
	Optical acquisition principle	TRIOS 3: confocal microscopy with ultrafast optical sectioning; Omnicam: active triangulation with continuous video capture
	Powder requirement	No surface powder required
Scanner calibration procedures	TRIOS 3 calibration	Calibration performed through the TRIOS software interface using the manufacturer-supplied calibration tip and calibration target. The scanner tip was mounted onto the calibration adapter, the calibration target inserted, and the calibration process initiated via the software. Calibration adjusts the scanner to factory reference settings. Manufacturer recommendations suggest performing calibration regularly (approximately every 7–8 days or after device movement or environmental changes).
	CEREC Omnicam calibration	Calibration performed using the Omnicam calibration tool provided by the manufacturer. The camera was inserted into the calibration device and the calibration workflow initiated within the CEREC software. The software guides the user through sequential calibration positions until the process reaches completion. This procedure ensures optimal optical accuracy before scanning.
Scanning protocol	Scan strategy	Standardized zigzag scanning path covering the entire arch
	Scanning starting point	Occlusal surfaces of the right posterior teeth
	Scan sequence	Occlusal surfaces → contralateral occlusal surfaces → buccal surfaces → palatal surfaces
	Scan body capture	Scan bodies rescanned from multiple angles to ensure complete geometry capture
	Scanning approach	Two-step scan: initial scan without scan bodies followed by scan with scan bodies attached
Scanning environment	Lighting conditions	Standardized ambient laboratory lighting
	Environmental temperature	Approximately 22–24 °C laboratory temperature
	Relative humidity	Approximately 40–60% relative humidity
	Surface characteristics	Matte resin casts to reduce optical reflections
Operator factors	Operator consistency	All scans performed by a single trained operator
	Operator experience	Operator experienced with both intraoral scanners
Scanning parameters	Scan resolution settings	Default manufacturer scanning resolution settings used for both scanners
	Average scanning time	Approximately 2–3 minutes per scan depending on scanner
	STL export settings	STL format exported using default scanner software tessellation parameters
Scanning repetitions	Number of scans per cast	12 scans per scanner per cast
	Total STL datasets	36 datasets per scanner across 3 angulation configurations
Data processing	Analysis software	GOM Inspect (GOM GmbH, Braunschweig, Germany)
	Alignment method	Scan-body-based best-fit alignment
	Geometric evaluation	Least-squares plane fitting and cylinder fitting to determine scan body axes and implant positions

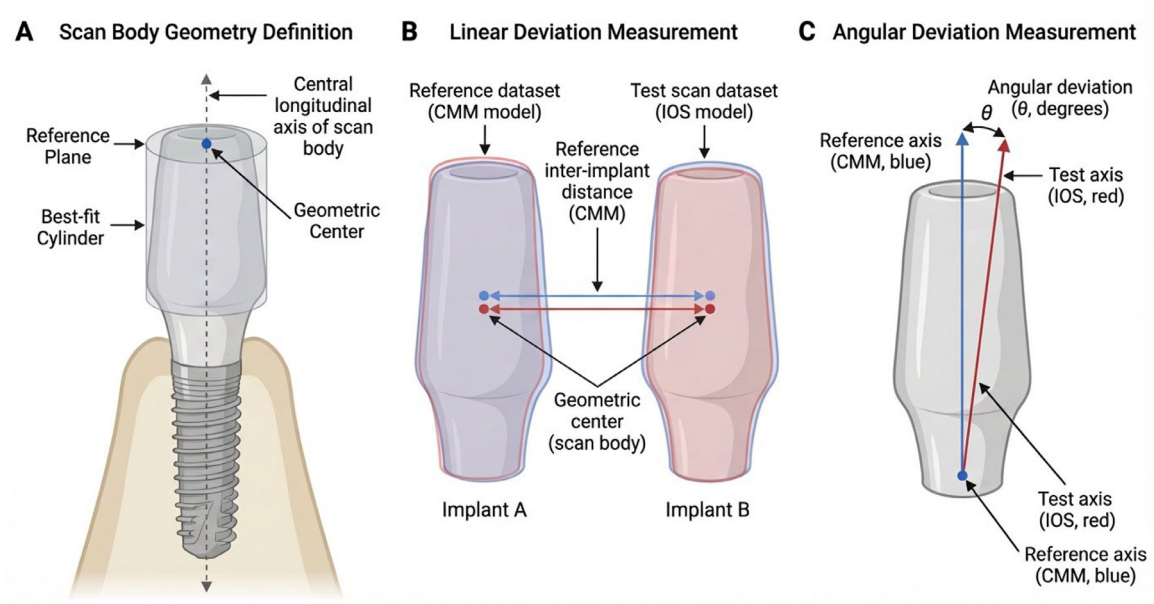


Fig. 2 – Workflow for calculating linear and angular deviations between reference and intraoral scan datasets. (A) Definition of scan body reference geometry used to determine implant position, including the reference plane, best-fit cylinder, central longitudinal axis, and geometric center of the scan body. (B) Linear deviation measurement calculated as the absolute difference between inter-implant distances measured between the geometric centers of the scan bodies in the reference (CMM) and intraoral scanner (IOS) datasets. (C) Angular deviation measurement calculated as the difference in orientation between the central longitudinal axes of the scan bodies in the reference and IOS datasets.

determined in both datasets, and the angular deviation was defined as the difference between these values expressed in degrees. This approach allowed simultaneous evaluation of translational discrepancies (changes in inter-implant distance) and rotational discrepancies (changes in implant axis orientation) (Figure 3). Analyses of the 2 implant pairs (A–B and C–D) were performed separately to explore potential effects related to scanner path progression, field-of-view variation, and cumulative stitching behavior during scanning.

Statistical analysis

All statistical analyses were performed using IBM SPSS Statistics for Windows, Version 24.0 (IBM Corp.). The Generalized Estimating Equations (GEE) method was used to assess the effects of implant angulation (cast), scanner type, and implant pair (A–B vs. C–D) on both inter-implant linear and angular deviation. The implant-pair factor was included as a within-cast variable to account for pair-specific variability in

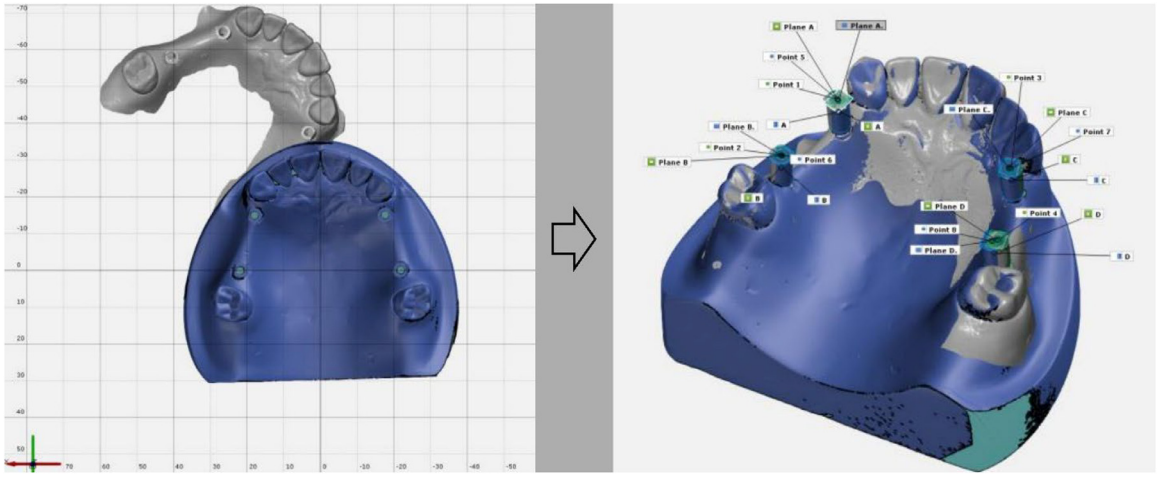


Fig. 3 – Superimposition and measurement workflow in GOM Inspect, showing the best-fit alignment of IOS scans to the CMM reference and the planes/axes used to calculate inter-implant linear and angular deviations.

the measured deviations within the same experimental cast. The GEE model was selected because the experiment involved repeated, correlated measurements (multiple scans per condition), and GEE provides robust population-averaged estimates without requiring the strict normality and sphericity assumptions of repeated-measures ANOVA.[33] An exchangeable (compound symmetry) correlation structure was assumed to model the correlation among repeated scans within the same cast–scanner combination. Parameter estimates (β coefficients), 95% confidence intervals (CIs), and p-values were reported. Least Significant Difference (LSD) post hoc tests were applied for pairwise comparisons when significant main or interaction effects were found. Interaction effects were excluded from the model when non-significant. Statistical significance was set at $p < .05$.

Results

Table 2 and Table 3 summarize pairwise comparisons of inter-implant linear and angular deviations across scanner type, cast model, and implant pair.

Linear deviations

The GEE model revealed a significant cast × scanner interaction for linear deviation, with an estimated effect size (β) of 0.028 (95% CI, 0.017 to 0.039; $p < .001$), indicating that the effect of scanner type on accuracy differed across implant angulations. In contrast, implant pair × scanner ($\beta = 0.002$; 95% CI, −0.021 to 0.024; $p = .914$) and cast × implant pair ($\beta = 0.009$; 95% CI, −0.007 to 0.024; $p = .264$) interactions were not significant. Interaction plots (Figure 4) illustrate that the 3Shape TRIOS 3 scanner exhibited greater deviation at lower angulations, whereas the CEREC Omnicam AC performed better in parallel implant configurations.

Table 2 – Pairwise comparison of mean inter-implant linear deviations (mm) according to scanner type, implant angulation (cast), and implant pair

Subgroup	Comparison	Mean difference (MD) (95% CI) [mm]	P-value
Cast 1 (0°)	3Shape TRIOS 3 vs CEREC Omnicam AC	0.029 (0.015 to 0.043)	<.001
Cast 2 (15°)	3Shape TRIOS 3 vs CEREC Omnicam AC	0.018 (0.001 to 0.034)	.038
Cast 3 (30°)	3Shape TRIOS 3 vs CEREC Omnicam AC	−0.027 (−0.052 to −0.002)	.037
3Shape TRIOS 3	Cast 1 vs Cast 2	0.031 (0.011 to 0.050)	.002
	Cast 1 vs Cast 3	0.048 (0.043 to 0.054)	<.001
	Cast 2 vs Cast 3	0.018 (−0.001 to 0.036)	.063
CEREC Omnicam AC	Cast 1 vs Cast 2	0.020 (0.003 to 0.037)	.024
	Cast 1 vs Cast 3	−0.008 (−0.028 to 0.013)	.469
	Cast 2 vs Cast 3	−0.027 (−0.056 to 0.001)	.062
Implant pair	A–B vs C–D	0.014 (0.003 to 0.024)	.009

Statistical model: Generalized Estimating Equations (GEE) model with Least Significant Difference (LSD) post hoc comparisons. Interaction terms: p (Cast × Scanner) < 0.001; p (Implant pair × Scanner) = 0.914; p (Cast × Implant pair) = 0.264. Abbreviations: MD = mean difference; CI = confidence interval.

Table 3 – Pairwise comparison of mean inter-implant angular deviations (°) according to implant angulation (cast), scanner type, and implant pair

Subgroup	Comparison	Mean difference (MD) (95 % CI) [°]	p-value
Cast (implant angulation)	1 vs 2	0.671 (0.292 to 1.050)	.001
	1 vs 3	0.585 (0.244 to 0.927)	.001
	2 vs 3	−0.085 (−0.197 to 0.026)	.134
Scanner type	3Shape TRIOS 3 vs CEREC Omnicam AC	−0.207 (−0.509 to 0.095)	.180
Implant pair	A–B vs C–D	0.060 (−0.158 to 0.277)	.590

Statistical model: Generalized Estimating Equations (GEE) with Least Significant Difference (LSD) post hoc comparisons. Interaction terms: p (Cast × Implant pair) = 0.858; p (Cast × Scanner) = 0.078; p (Implant pair × Scanner) = 0.384. Abbreviations: MD = mean difference; CI = confidence interval.

Table 2 presents the GEE results for inter-implant linear deviations. A significant interaction effect between cast and scanner type was detected ($p < .001$). Therefore, post hoc LSD pairwise comparisons were performed within each scanner and cast.

Pairwise analysis revealed that in Cast 1 (0°) and Cast 2 (15°), the mean linear deviation obtained with the 3Shape TRIOS 3 scanner was significantly higher than that of the CEREC Omnicam AC scanner (mean differences = 0.029 mm, $p < .001$; and .018 mm, $p = .038$, respectively). Conversely, in Cast 3 (30°), the 3Shape TRIOS 3 demonstrated significantly lower mean deviation than CEREC Omnicam AC (mean difference = −0.027 mm, $p = .037$) (Figure 4).

Within the 3Shape TRIOS 3 group, linear deviations in Cast 1 were significantly higher than in Cast 2 (mean difference = 0.031 mm, $p = .002$) and Cast 3 (mean difference = 0.048 mm, $p < .001$), while no significant difference was found between Cast 2 and Cast 3. In the CEREC Omnicam AC group, Cast 1 also exhibited greater mean deviation than Cast 2 (mean difference = 0.020 mm, $p = .024$), whereas no significant difference was detected between Cast 3 and either of the other casts (Figure 4).

The implant pair effect (A–B vs. C–D) did not interact significantly with scanner type or cast. However, independent of these factors, the mean linear deviation in the A–B implant pair was significantly higher than in the C–D implant pair by approximately 0.014 mm ($p = .009$) (Figure 5A).

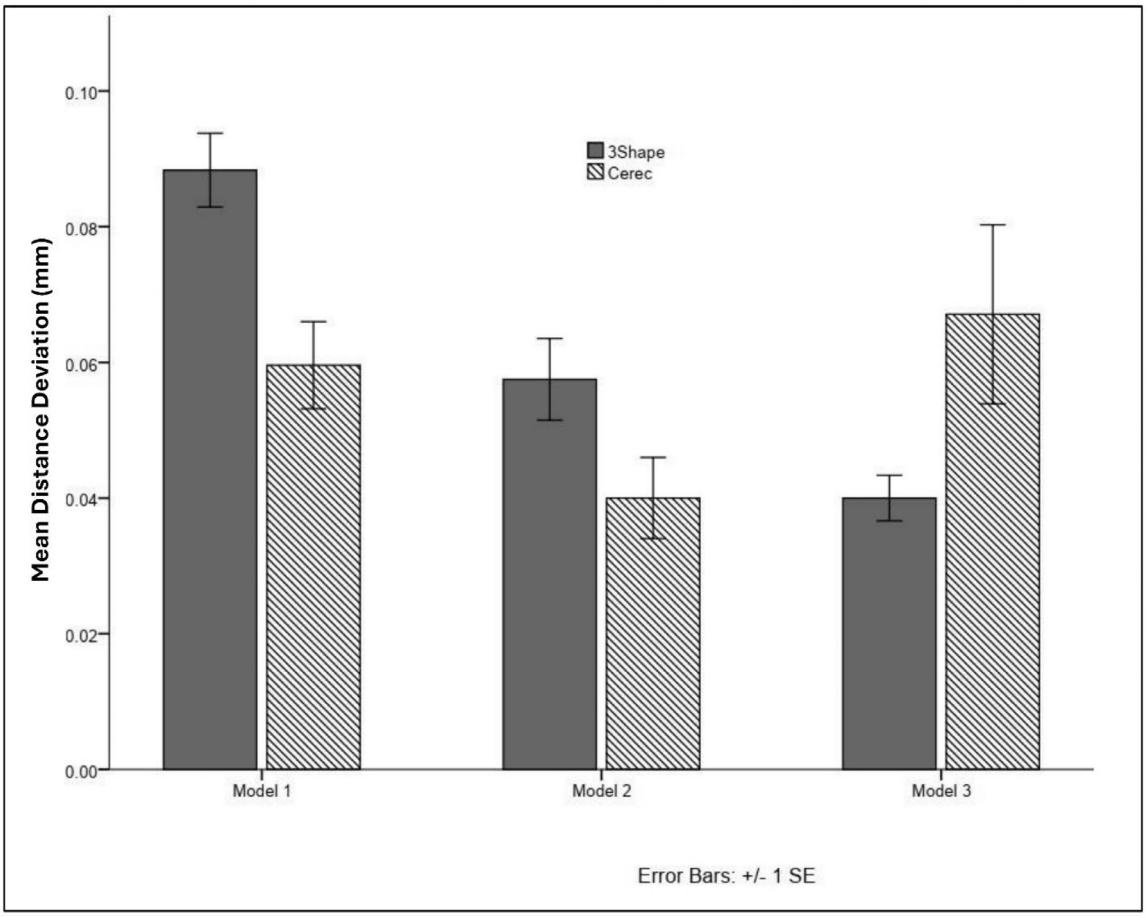


Fig. 4 – Mean inter-implant linear deviation (mm) for 3Shape TRIOS 3 and CEREC Omnicam AC across Casts 1–3. Error bars represent ±1 SE.

Angular deviations

For angular deviation, no significant cast × scanner interaction was detected (β = 0.017; 95% CI, −0.008 to 0.043; p = .078). The main effect of implant angulation was significant (β = −0.628; 95% CI, −0.917 to −0.338; p = .001), indicating reduced angular deviation with increasing implant angulation. Interaction plots (Figure 5B) further confirm a decreasing trend in angular error from 0° to 30° across scanner types.

As shown in Table 3, no significant interaction among cast, implant pair, and scanner type was detected (p > .05). Therefore, the main effects were interpreted independently. The mean angular deviation in Cast 1 (0°) was significantly greater than in Cast 2 (15°) and Cast 3 (30°) by approximately 0.671° (p = .001) and 0.585° (p = .001), respectively (Figure 5 B). No significant difference in angular deviation was found between Cast 2 and Cast 3 (p = .134).

Scanner type (3Shape TRIOS 3 vs. CEREC Omnicam AC) and implant pair (A–B vs. C–D) had no statistically significant effects on angular deviation (p = .180 and p = .590, respectively) (Figures 5C and D).

Discussion

This in vitro study evaluated the influence of implant angulation on the linear and angular accuracy of digital impressions for three-unit implant-supported fixed partial dentures obtained with 2 intraoral scanners, CEREC Omnicam AC and 3Shape TRIOS 3. The results demonstrated that implant angulation significantly influenced both linear and angular deviations, while a significant interaction between scanner type and angulation affected linear accuracy. The TRIOS 3 scanner showed superior accuracy for 30° angulated implants, whereas CEREC Omnicam AC performed better for 0° and 15° casts. No significant difference in angular accuracy was observed between scanners or between the 2 implant pairs (A–B and C–D). Based on these findings, the null hypothesis—that implant angulation and scanner type would not affect digital impression accuracy—was partially rejected. The originality of the present study lies in the evaluation of implant angulation, specifically in a short-span three-unit implant-supported restoration model, with simultaneous assessment of both linear and angular deviations using 2 intraoral scanners based on different optical principles. This design allowed the influence of implant angulation to be interpreted not only in terms of scanner performance but also in relation to the underlying scanning mechanism, within a clinically relevant and standardized experimental configuration.

As implant angulation increased, linear deviations decreased, and angular deviations improved. From a

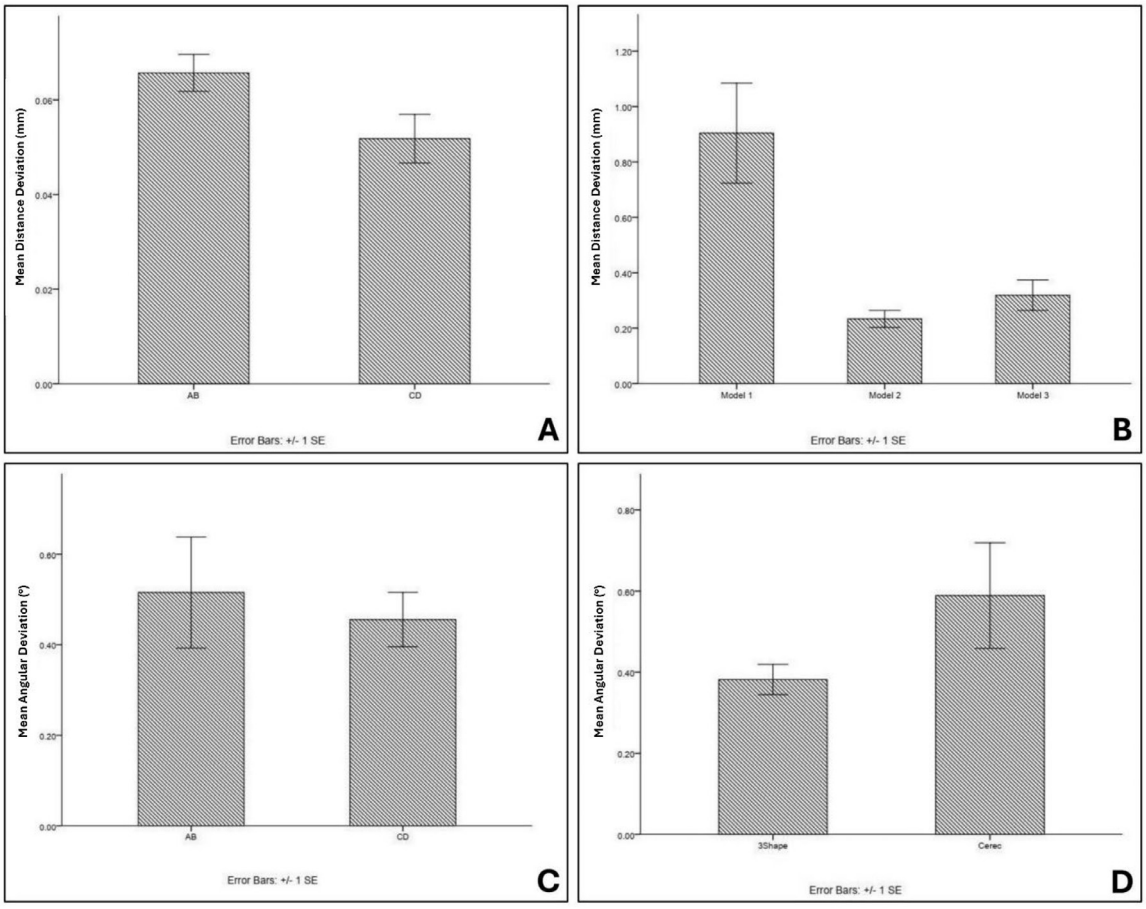


Fig. 5 – Linear and angular deviation outcomes by implant pair, cast, and scanner type. A: Mean linear deviation by implant pair (A–B vs. C–D). B: Mean angular deviation by cast (0°, 15°, 30°). C: Mean angular deviation by implant pair. D: Mean angular deviation by scanner type. Error bars represent ±1 SE.

technical perspective, this behavior can be explained by the principles of geometric and optical scanning. Parallel implants generate overlapping reflective surfaces with limited geometric differentiation, providing fewer distinct reference cues for the scanner's alignment and stitching algorithms. Consequently, similar surface features may be more difficult to distinguish, thereby increasing linear deviation. In contrast, greater implant divergence enhances spatial separation and optical accessibility of the scan bodies, allowing the acquisition of more unique topographic information and reducing cumulative error. Angulated implants also expose a larger portion of their surface to the scanner's line of sight, improving triangulation and reducing linear and angular discrepancies.[29] The observed improvement in angular accuracy with higher implant divergence is likely related to the capture of more distinctive optical reference cues at steeper angulations, particularly from the bevel and cylindrical surfaces of the scan bodies, which facilitates more precise reconstruction of the longitudinal axis.[34,35] In addition, this effect is likely influenced by scanner-specific reconstruction algorithms, as different intraoral scanners use distinct image acquisition and surface-matching strategies. Scan body geometry may also contribute to this behavior, as parallel cylindrical surfaces provide fewer distinctive landmarks for registration than more spatially separated angulated scan bodies. Importantly, these findings should not be interpreted as a recommendation to intentionally place implants with greater angulation to enhance digital impression accuracy. In clinical practice, implant angulation is primarily dictated by anatomical, biological, and biomechanical considerations, and parallel implant placement remains the preferred goal whenever feasible. Rather, the present results indicate that when implants must be placed at an angle for valid clinical reasons, their digitalization using intraoral scanners is not compromised and may remain reliable within short-span configurations.

The present findings are consistent with earlier studies reporting better accuracy in inclined implants. Lin et al. showed that divergent implants increased scanning accuracy until a threshold of approximately 30°, after which improvements plateaued.[26] Lee et al.[9] reported that mesially tilted terminal implants improved accuracy, while Zhang et al.[27] and Arshad et al.[28] found that rotational and linear deviations decreased as inter-implant divergence increased when using 3Shape and Sirona scanners. Collectively, these studies confirm that moderate divergence enhances spatial recognition and improves the stitching accuracy of digital datasets. However, the results of the present study contrast with those of

Kurtulmus-Yilmaz et al.[36] and Gómez-Polo et al.,[32] who concluded that parallel implants achieved higher accuracy than angulated ones. These discrepancies may stem from differences in experimental configuration. Gómez-Polo et al.[32] used a complete-arch cast with 4 implants and 5 different scan body bevel orientations, where cumulative stitching errors likely magnified inaccuracies toward the distal regions of the arch. In contrast, the present study analysed short-span, 3-unit restorations, where such error propagation is limited. Moreover, the scanner movement pattern and starting point differ between full-arch and short-span scans; in full-arch scanning, data accumulation from one end to the other can lead to asymmetric distortion, explaining why implants at the end of the scan showed higher deviation. The current study controlled this variable by scanning both sides symmetrically, minimizing directional distortion. The optical exposure angle also differs between studies: in the present experiment, angulated scan bodies were oriented buccally, improving surface visibility, whereas Gómez-Polo's facial and distal bevel positions may have reflected light less effectively toward the sensor. These methodological distinctions explain the contrasting outcomes. The study by Taghva et al.[29] also complements our findings. They demonstrated that implant depth significantly affects accuracy, with shallow (1 mm) and deep (4 mm) implants showing higher accuracy than intermediate depths. This supports the present observation that optical accessibility, whether through vertical (depth) or angular (inclination) positioning, directly influences scanning accuracy. Reduced visibility or partial obstruction of the scan body surface can decrease data quality and increase alignment errors, highlighting the shared geometric principle that the more visible the scan body, the higher the accuracy. Several earlier studies further corroborate these trends. Arshad et al.[28] observed that rotational displacement errors decreased with increasing inter-implant angles. In contrast, Basaki et al.[37] and Alikhasi et al.[38] reported that implant angulation up to 45° did not significantly affect accuracy, suggesting that beyond a moderate divergence, accuracy may stabilize. Such differences likely result from variations in scanning systems, the number of implants, and superimposition algorithms. The present study used best-fit alignment of entire scan body geometries in GOM Inspect, whereas other studies used limited reference-point alignment, potentially underestimating geometric deviation.[34]

The interaction between scanner type and angulation indicates that scanner technology determines optimal performance conditions.[39] The CEREC Omnicam AC, based on continuous video-based active triangulation, captures data most accurately from surfaces perpendicular to the light source and evenly illuminated—conditions best met by parallel or mildly angulated implants. Conversely, TRIOS 3, which employs confocal microscopy and ultrafast optical sectioning, performs optimally when multiple depth and inclination cues are available. This explains why TRIOS 3 showed superior accuracy for 30° implants, as its depth-sensing algorithm benefits from increased surface variation. These findings are consistent with Cakmak et al.[40] who found that while all current IOSs produce clinically acceptable accuracy, variations in scanning technology and scan body geometry can produce subtle differences under specific conditions. In addition, scan body geometry and surface orientation may influence optical data capture, as increased divergence exposes a larger portion of the scan body surface to the scanner's optical field, improving feature recognition and potentially contributing to the reduced angular deviations observed in the present study.

The magnitude of deviations observed in this study should be interpreted in the context of previously reported in vitro data. Prior investigations have documented inter-implant linear deviations ranging from approximately 6 μm to 337 μm and angular discrepancies ranging from 0.07° to 0.3° for IOS –based implant impressions.[41] In the present investigation, linear deviations were higher, ranging from approximately 500 to 675 μm, whereas angular deviations were comparatively small (approximately 0.05°–0.06°). These findings indicate that, while greater linear discrepancies were observed relative to many earlier in vitro reports, angular accuracy remained comparable to or lower than previously reported values. It should be noted that most tolerance values reported in the implant prosthodontic literature refer to prosthesis misfit at the implant–abutment interface, rather than to linear or angular deviations derived from digital impression accuracy analyses. The current literature provides limited evidence for defining a universally accepted clinical threshold for acceptable misfit, largely due to variations in study designs, measurement methods, and reported outcomes. Previous reports suggest that vertical prosthetic misfits ranging from approximately 30 μm to 160 μm and horizontal misfits of approximately 150 μm did not consistently result in mechanical complications, whereas tolerable limits for biological outcomes appear to be considerably larger.[42] Additionally, vertical misfits of approximately 466 μm to 1 mm and horizontal discrepancies of approximately 345 μm have been reported without clear adverse biological effects.[42] Importantly, these values correspond to prosthetic misfit following prosthesis fabrication and cannot be directly extrapolated to the linear and angular deviations measured at the digital impression stage. Given the absence of universally established clinical thresholds for acceptable linear and angular deviations in implant prosthodontics,[43] the results should be interpreted comparatively rather than normatively.

The absence of a significant difference between implant pairs A–B and C–D suggests that, within the limits of this short-span experimental setup, scanner path progression and field-of-view–related effects did not produce detectable differences in accuracy. In contrast, Gómez-Polo et al.[32] reported increased distortion in implants located at the end of the scan path in full-arch casts. This discrepancy indicates that scanning span length plays a major role in cumulative error propagation, underscoring the need for caution when extrapolating short-span results to full-arch restoration.

Within the limitations of this in vitro study, the results suggest that moderate implant angulations (15°-30°) do not adversely affect the accuracy of intraoral scanner–based digital impressions in short-span implant-supported restorations. Under the experimental conditions evaluated, both intraoral scanners demonstrated comparable linear and angular deviation patterns across different angulation configurations, indicating that moderate divergence between implants does not inherently compromise digital impression

accuracy. These findings may be clinically relevant in situations where implant angulation is dictated by anatomical, surgical, or prosthetic constraints.

The present study has inherent limitations. As an in vitro investigation, it was performed under idealized conditions without intraoral variables such as saliva, limited access, patient movement, or variable lighting, all of which may influence scan quality in clinical settings.[35] Furthermore, the casts simulated only 3-unit fixed partial dentures with implants placed in the premolar–molar region, which may limit extrapolation of the findings to other clinical situations involving different implant distributions or longer edentulous spans. Longer spans are particularly susceptible to cumulative stitching errors as the scanning distance increases and the number of anatomical reference points decreases.[40] Only 2 intraoral scanners were evaluated, and the results may therefore not be generalizable to other scanning systems that use different optical acquisition principles or software reconstruction algorithms. In addition, the study employed a single scan body design and material, which may influence optical capture characteristics and geometric feature recognition by intraoral scanners. Different scan body geometries or surface properties could potentially affect digital impression accuracy. Another limitation is that superimposition was performed using the full scan body surface geometry, which may be influenced by scanner-dependent resolution and surface sampling characteristics. In addition, consistent buccal orientation of the scan body bevel and reduced accessibility of interproximal scan body surfaces—particularly in angulated configurations—may affect local surface capture. However, because identical scan bodies, orientations, and alignment procedures were used for all experimental groups and both scanners, such effects would be systematic rather than selective, and therefore unlikely to bias comparative analyses between scanners or implant angulations. Even so, the present results should be interpreted with caution, as clinical fit, biological outcomes, and long-span or full-arch restorations were not assessed. Future research should include in vivo studies evaluating the combined influence of implant angulation, scan body geometry, bevel orientation, scanning depth, and scanning strategy across various clinical conditions and full-arch scenarios.

Conclusions

Based on the findings of this in vitro study, it could be concluded that:

1. Implant angulation significantly influenced the accuracy of digital impressions, with angular and linear deviations differing between parallel and moderately angulated implant configurations.
2. A significant interaction between scanner type and implant angulation was observed for inter-implant linear deviations, with the CEREC Omnicam AC demonstrating lower linear deviations at 0° and 15° angulations, and the 3Shape TRIOS 3 demonstrating lower linear deviations at 30° angulations.
3. Scanner type and implant pair (A–B vs. C–D) did not significantly affect angular deviations, indicating comparable angular accuracy between the evaluated intraoral scanners within short-span implant configurations.
4. From a clinical standpoint, the results suggest that moderate implant angulations (15°–30°) do not result in reduced accuracy of intraoral scanner–based digital impressions in short-span implant-supported restorations.

Ethical approval

The Research Ethics Committee of Tehran University of Medical Sciences authorized the present study (IR.TUMS.DENTISTRY.REC.1397.4922).

Funding

This research did not receive any specific grant from funding agencies in the public, commercial, or not-for-profit sectors.

Informed consent statement

Not applicable.

Consent for publication

Not applicable.

Author contributions

Conceptualization: N.A., M.A., and S.H.; Methodology: N.A., M.A., and S.H.; Software: S.A.M.; Validation: M.A. and S.H.; Formal analysis: M.A. and S.H.; Investigation: M.GH.; Resources: N.A. and S.H.; Data curation: M.GH. and S.A.M.; Writing—original draft preparation: M.A.; Writing—review and editing: N.A., S.H., and S.A.M.; Visualization: S.A.M. and M.A.; Supervision: N.A. and S.H.; Project administration: S.H. All authors have read and approved the final version of the manuscript.

Conflict of interest

None disclosed.

REFERENCES

1. Mosaddad SA, Talebi S, Keyhan SO, et al. Dental implant considerations in patients with systemic diseases: an updated comprehensive review. J Oral Rehabil 2024;51:1250–302.
2. Sadek HS, Anany NM, El-Anwar MI, et al. Biomechanical performance of implant-tooth-supported prostheses: a numerical 3D finite element analysis. Int Dent J 2025;75:103882.
3. Sahin S, Cehreli MC. The significance of passive framework fit in implant prosthodontics: current status. Implant Dent 2001;10:85–92.

4. Couso-Queiruga E, Ramseier CA, Chappuis V, M S, Buser D, Brägger U, Salvi GE. Impact of marginal misfit in implant-supported fixed dental prostheses on peri-implant bone levels: a retrospective quantitative analysis. Clin Oral Implants Res 2026;37:69–78.
5. Katsoulis J, Takeichi T, Sol Gaviria A, Peter L, Katsoulis K. Misfit of implant prostheses and its impact on clinical outcomes. Definition, assessment and a systematic review of the literature. Eur J Oral Implantol 2017;10(Suppl 1):121–38.
6. Habibzadeh S, Ghodsi S, Alikhasi M, Mosaddad SA, Mohebbi H. Abutment connection structural changes in dual-retained and screw-retained metal-ceramic implant-supported restorations: an in vitro study, part I. BMC Oral Health 2025;25:667.
7. Rutkunas V, Larsson C, Vult von Steyern P, Mangano F, Gedrimiene A. Clinical and laboratory passive fit assessment of implant-supported zirconia restorations fabricated using conventional and digital workflow. Clin Implant Dent Relat Res 2020;22:237–45.
8. Stefos S, Kourtis S, Sarafianou A, Zoidis P. The influence of impression material on the accuracy of the master cast in implant restorations. Open Dent J 2018;12:1123–36.
9. Lee JH, Bae JH, SY Lee. Trueness of digital implant impressions based on implant angulation and scan body materials. Sci Rep 2021;11:21892.
10. Christensen GJ. Impressions are changing: deciding on conventional, digital or digital plus in-office milling. J Am Dent Assoc 2009;140:1301–4.
11. Muslu T, Kurtulmus-Yilmaz S. Effect of implant angulation on the trueness and precision of intraoral scanning and photogrammetry. BMC Oral Health 2025;25:1739.
12. D'Ambrosio F, Giordano F, Sangiovanni G, Di Palo MP, Amato M. Conventional versus digital dental impression techniques: what is the future? An Umbrella Review. Prosthesis 2023;5:851–75.
13. Grande F, Nuytens P, Zahabiyoun S, Iocca O, Catapano S, Mijiritsky E. Factors influencing the intraoral implant scan accuracy: a review of the literature. J Dent 2025;161:105973.
14. Borşanu I-A, Rusu L-C, Antonie S-M, Bratu E-A. Comparative clinical evaluation of digital versus conventional dental impression techniques in implant-supported restorations. Prosthesis 2025;7:135.
15. Eggmann F, Blatz MB. Recent advances in intraoral scanners. J Dent Res 2024;103:1349–57.
16. Kafedzhieva A, Vlahova A, Chuchulska B. Digital technologies in implantology: a narrative review. Bioengineering 2025;12:927.
17. Chatborirak P, Phannarus K, Kanpittaya P, Chantarawaratit PO. The accuracy and trueness of intraoral scanners in neonates with cleft lip and palate: a comparison of 3d digital models. Int Dent J 2025;75:100834.
18. Choi JH, Lim YJ, Yim SH, Kim CW. Evaluation of the accuracy of implant-level impression techniques for internal-connection implant prostheses in parallel and divergent models. Int J Oral Maxillofac Implants 2007;22:761–8.
19. Jo SH, Kim KI, Seo JM, Song KY, Park JM, Ahn SG. Effect of impression coping and implant angulation on the accuracy of implant impressions: an in vitro study. J Adv Prosthodont 2010;2:128–33.
20. Conrad HJ, Pesun IJ, DeLong R, Hodges JS. Accuracy of two impression techniques with angulated implants. J Prosthet Dent 2007;97:349–56.
21. Arezoobakhsh A, Shayegh SS, Jamali Ghomi A, Hakimaneh SMR. Comparison of marginal and internal fit of 3-unit zirconia frameworks fabricated with CAD-CAM technology using direct and indirect digital scans. J Prosthet Dent 2020;123:105–12.
22. Mangano FG, Hauschild U, Veronesi G, Imburgia M, Mangano C, Admakin O. Trueness and precision of 5 intraoral scanners in the impressions of single and multiple implants: a comparative in vitro study. BMC Oral Health 2019;19:101.
23. Imburgia M, Logozzo S, Hauschild U, Veronesi G, Mangano C, Mangano FG. Accuracy of four intraoral scanners in oral implantology: a comparative in vitro study. BMC Oral Health 2017;17:92.
24. Önöral Ö, Kurtulmus-Yilmaz S, Toksoy D, Ozan O. Effect of angulation on the 3D trueness of conventional and digital implant impressions for multi-unit restorations. J Adv Prosthodont 2023;15:290–301.
25. Taruna M, Chittaranjan B, Sudheer N, Tella S, Abusaad M. Prosthodontic perspective to all-on-4® concept for dental implants. J Clin Diagn Res 2014;8:Ze16–9.
26. Lin WS, Harris BT, Elathamna EN, Abdel-Azim T, Morton D. Effect of implant divergence on the accuracy of definitive casts created from traditional and digital implant-level impressions: an in vitro comparative study. Int J Oral Maxillofac Implants 2015;30:102–9.
27. Zhang YJ, Qiao SC, Qian SJ, Zhang CN, Shi JY, Lai HC. Influence of different factors on the accuracy of digital impressions of multiple implants: an in vitro study. Int J Oral Maxillofac Implants 2021;36:442–9.
28. Arshad M, Asgari A, Kharazifard MJ, Ameri N. Effect of implant angulation on the rotational displacement of a 3-unit bridge after digital impression. Int J Dent 2022;2022:8634091.
29. Taghva M, Mosaddad SA, Ansarifard E, Sadeghi M. Could various angulated implant depths affect the positional accuracy of digital impressions? An in vitro study. J Prosthodont 2024;33:791–800.
30. Mohammed BA, Jalal RA. Comparative analysis of implant deviation with varying angulations and lengths using a surgical guide: an in vitro experimental study. Prosthesis 2025;7:125.
31. Giménez B, Özcan M, Martínez-Rus F, Pradíes G. Accuracy of a digital impression system based on active wavefront sampling technology for implants considering operator experience, implant angulation, and depth. Clin Implant Dent Relat Res 2015;17(Suppl 1):e54–64.
32. Gómez-Polo M, Cascos R, Ortega R, Barmak AB, Kois JC, Pérez-Barquero JA, Revilla-León M. Influence of scanning pattern on accuracy, time, and number of photograms of complete-arch implant scans: a clinical study. J Dent 2024;150:105310.
33. Ziegler A, Vens M. Generalized estimating equations. Notes on the choice of the working correlation matrix. Methods Inf Med 2010;49:421–5 discussion 6-32.
34. Kihara H, Hatakeyama W, Komine F, et al. Accuracy and practicality of intraoral scanner in dentistry: a literature review. J Prosthodont Res 2020;64:109–13.
35. Revilla-León M, Lanis A, Yilmaz B, Kois JC, Gallucci GO. Intraoral digital implant scans: parameters to improve accuracy. J Prosthodont 2023;32:150–64.
36. Kurtulmus-Yilmaz S, Ozan O, Ozcelik TB, Yagiz A. Digital evaluation of the accuracy of impression techniques and materials in angulated implants. J Dent 2014;42:1551–9.
37. Basaki K, Alkumru H, De Souza G, Finer Y. Accuracy of digital vs conventional implant impression approach: a three-dimensional comparative in vitro analysis. Int J Oral Maxillofac Implants 2017;32:792–9.
38. Alikhasi M, Siadat H, Nasirpour A, Hasanzade M. Three-dimensional accuracy of digital impression versus conventional method: effect of implant angulation and connection type. Int J Dent 2018;2018:3761750.
39. García-Gil I, Cortés-Bretón-Brinkmann J, Jiménez-García J, Peláez-Rico J, MJ Suárez-García. Precision and practical usefulness of intraoral scanners in implant dentistry: a systematic literature review. J Clin Exp Dent 2020;12:e784–e93.
40. Çakmak G, Yilmaz H, Treviño Santos A, Kökat AM, Yilmaz B. Effect of scanner type and scan body location on the accuracy

of mandibular complete-arch digital implant scans: an in vitro study. J Prosthodont 2022;31:419–26.
41. Rutkūnas V, Gečiauskaitė A, Jegelevičius D, Vaitiekūnas M. Accuracy of digital implant impressions with intraoral scanners. A systematic review. Eur J Oral Implantol 2017;10(Suppl 1): 101–20.
42. Abdelrehim A, Etajuri EA, Sulaiman E, Sofian H, Salleh NM. Magnitude of misfit threshold in implant-supported restorations: a systematic review. J Prosthet Dent 2024;132:528–35.
43. Mosaddad SA. Standardizing methodologies in prosthodontics to improve research reliability and peer review efficiency: a perspective-based proposal. Health Sci Rep 2025;8:e71547.